Rotational hybridization, and control of alignment and orientation in triatomic ultralong-range Rydberg molecules

2015 New J. Phys. 17 013021

(http://iopscience.iop.org/1367-2630/17/1/013021)

New Journal of Physics
The open access journal at the forefront of physics

Deutsche Physikalische Gesellschaft DPG
IOP Institute of Physics

Published in partnership with: Deutsche Physikalische Gesellschaft and the Institute of Physics

OPEN ACCESS

RECEIVED
24 June 2014

ACCEPTED FOR PUBLICATION
3 December 2014

PUBLISHED
15 January 2015

PAPER

Rotational hybridization, and control of alignment and orientation in triatomic ultralong-range Rydberg molecules

Rosario González-Férez[1,2], **H R Sadeghpour**[3] **and Peter Schmelcher**[2,4]

[1] Instituto Carlos I de Física Teórica y Computacional, and Departamento de Física Atómica, Molecular y Nuclear, Universidad de Granada, E-18071 Granada, Spain
[2] The Hamburg Center for Ultrafast Imaging, Luruper Chaussee 149, D-22761 Hamburg, Germany
[3] ITAMP, Harvard-Smithsonian Center for Astrophysics, Cambridge, MA 02138, USA
[4] Zentrum für Optische Quantentechnologien, Universität Hamburg, Luruper Chaussee 149, D-22761 Hamburg, Germany

E-mail: rogonzal@ugr.es

Keywords: Rydberg molecules, electric field, control of alignment and orientation, ultralong-range

Abstract

We explore the electronic structure and rovibrational properties of an ultralong-range triatomic Rydberg molecule formed by a Rydberg atom and a ground state heteronuclear diatomic molecule. We focus here on the interaction of a Rb(n, $l \geqslant 3$) Rydberg atom with a KRb($N=0$) diatomic polar molecule. There is significant electronic hybridization with the Rb($n=24, l \geqslant 3$) degenerate manifold. The polar diatomic molecule is allowed to rotate in the electric fields generated by the Rydberg electron and core as well as an external field. We investigate the metamorphosis of the Born–Oppenheimer potential curves, essential for the binding of the molecule, with varying electric field and analyze the resulting properties such as the vibrational structure and the alignment and orientation of the polar diatomic molecule.

1. Introduction

While in the early years of Rydberg physics there was a substantial focus on high resolution spectroscopy [1] the advent of Bose–Einstein condensation [2] has brought Rydberg atoms and molecules into the focus of fields that were previously not considering these highly excited and fragile quantum objects. This includes ultracold Rydberg gases and plasmas [3, 4], quantum optics and many-body physics of long-range interacting Rydberg systems [4], quantum simulators [5] as well as quantum information processing based on entanglement generation between interacting Rydberg atoms in optical lattices [6]. A recent spectacular development is the prediction [7] and experimental detection [8] of ultralong-range molecules from an ultracold atomic cloud. Opposite to the well-known Rydberg molecules with a tightly bound positively charged core and an electron circulating around it, the ultralong-range molecular species follows a very different bonding mechanism with, for a diatomic molecule, internuclear distances of the order of the extension of the electronic Rydberg state. Here, a ground state atom locally probes the Rydberg electronic wavefunction whose interaction is typically described by s- and p-wave Fermi-type pseudopotentials [9, 10]. The latter leads to the unusual oscillatory behavior of the corresponding adiabatic potential energy curves and a correspondingly rich vibrational dynamics. For principal quantum numbers of typically $n \approx 30$–100, being routinely prepared in the experiments, the diatomic molecules can be up to a few μm in size. These exotic species were first predicted theoretically back in 2000 by Greene *et al* [7] providing polar (trilobite) and non-polar states with vibrational binding energies in the GHz and MHz regimes, respectively. Beyond the detection of non-polar ultralong-range molecules and their spectroscopic characterization, Rydberg triatomic molecules and excited diatomic molecules bound by quantum reflection have been found [11].

The sensitivity of Rydberg atoms to external fields carries over also to ultralong-range Rydberg molecules which opens unprecedented opportunities for their weak field control. This includes static magnetic and electric fields or laser fields which could be used to change the electronic structure severely and correspondingly change

the molecular geometry and rovibrational dynamics. Electric and magnetic field control of molecular binding properties [12–14] as well as alignment have been demonstrated very recently [15].

If the neutral ground state atom immersed into the Rydberg wave function is replaced by a Λ-doublet heteronuclear diatomic molecule [16–18], giant polyatomic Rydberg molecules can form. These triatomic ultralong-range Rydberg molecules could be created in an ultracold mixture of atoms and molecules by using standard Rydberg excitation schemes. The Rydberg electron is coupled to the two internal states of the polar ground state molecule, creating a series of undulating Born–Oppenheimer potential (BOP) curves due to the oscillating character of the Rydberg electron wave functions. The electronic structure of these giant molecules could be easily manipulated by means of electric fields of a few V cm^{-1}, creating a complex set of avoided crossings among neighboring levels. In particular a Raman scheme to couple the two internal states of opposite orientation of the polar diatomic molecule has been proposed [16].

In this work, we consider a triatomic molecule formed by a Rb Rydberg atom and a ground state KRb polar molecule. Compared to previous works [16–18], we perform an extended and realistic treatment of the internal motion of the diatomic molecule. Indeed, we explicitly introduce the angular degrees of freedom of the diatomic molecule and as such are capable of describing properly the molecular rotational motion in the rigid rotor approximation. The free rotation of the diatomic molecule in the triatomic Rydberg molecule is now dressed due to the combined electric fields of the Rydberg electron and the core, and is characterized by a strong orientation and alignment along the field direction. Since the permanent dipole moment of the molecule is not fixed in space but rotates, we include in our description the three components of the electric field induced by the Rydberg atom. We analyze the BOP of the Rb($n, l \geqslant 3$)-KRb Rydberg triatomic molecule as the internuclear separation between KRb and the Rb^+ core varies and explore in detail the effects of the electric field induced by the Rydberg atom on the rotational motion of KRb, by studying the hybridization of its angular motion, orientation and alignment. We also investigate the impact of an additional electric field on these BOPs and their vibrational spectrum.

The paper is organized as follows: in section 2 we describe the Hamiltonian of the system and the electric field induced by the Rydberg core and electron in the diatomic molecule. The BOP as a function of the distance between the perturbing diatomic molecule and the Rydberg core as well as the resulting alignment and orientation of the diatomic molecule are presented in section 3. In section 4, we focus on the impact of an external field. The vibrational spectrum of the Rydberg triatomic molecule is discussed in detail in section 5 and the conclusions are provided in section 6.

2. Hamiltonian, interactions and computational approach

We consider a triatomic molecule formed by a Rydberg atom and a ground state heteronuclear diatomic molecule in an electric field. The permanent electric dipole moment of the polar molecule interacts with the electric field provided by the Rydberg core and electron as well as the external electric field. With increasing electric field strength the rotational motion becomes a librating one which leads to the alignment and orientation of the molecular axis. Here, we describe the diatomic molecule by means of a rigid rotor approach. This should be a good approximation for the tightly bound molecule since we are allowed to adiabatically separate the rotational and vibrational motions even in the presence of the electric field induced by the Rydberg atom [19, 20].

For the sake of simplicity, we fix the geometry of the Rydberg triatomic molecule: the laboratory fixed frame (LFF) is defined so that the Rydberg core is located in its origin, and the diatomic molecule is on the Z-axis at a distance R. A qualitative sketch is presented in figure 1. The positions of the diatomic molecule and electron in the LFF are $\mathbf{R} = R\hat{Z}$ and $\mathbf{r} = (r\hat{R}, \theta_r\hat{\theta}, \phi_r\hat{\phi})$, respectively.

Within the Born–Oppenheimer approximation, the adiabatic Hamiltonian of this system is given by

$$H_{\rm ad} = H_A + H_{\rm mol} + H_{\rm ext}. \tag{1}$$

The first term stands for the single electron Hamiltonian describing the Rydberg atom

$$H_A = -\frac{\hbar^2}{2m_e}\nabla_r^2 + V_l(r) \tag{2}$$

with $V_l(r)$ being the l-dependent model potential where l is the angular momentum quantum number of the Rydberg electron

$$V_l(r) = -\frac{Z_l(r)}{r} - \frac{\alpha_c}{2r^4}\left[1 - e^{-(r/r_c)^6}\right],$$

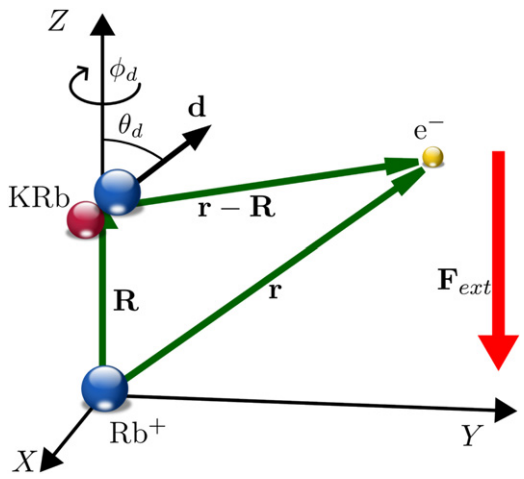

Figure 1. A sketch (not to scale) of the triatomic molecule formed by the Rydberg atom and diatomic polar molecule.

where $Z_l(r)$ is an effective charge, α_c the static dipole polarizability of the positive-ion core and r_c is a cutoff radius [21].

The second term $H_{\rm mol}$ is the Hamiltonian of the polar molecule in the electric field created by the Rydberg electron and core, $\mathbf{F}_{\rm ryd}(\mathbf{R},\,\mathbf{r})$. In the rigid rotor approximation, the molecular Hamiltonian reads

$$H_{\rm mol} = B\mathbf{N}^2 - \mathbf{d}\cdot\mathbf{F}_{\rm ryd}(\mathbf{R},\,\mathbf{r}) \tag{3}$$

with B being the rotational constant, $\mathbf{N}$ the molecular angular momentum operator and $\mathbf{d}$ the permanent electric dipole moment of the diatomic molecule, which is parallel to the molecular internuclear axis. Note that the internal rotational motion of the diatomic molecule is described by the Euler angles $\Omega_d = (\theta_d,\,\phi_d)$, which relate the diatomic molecular fixed frame (MFF) and LFF. The MFF is defined with its origin at the center of mass of the two nuclei of this diatomic molecule and the Z_M-axis being along the internuclear axis. The electric field due to the Rydberg electron and core is given by

$$\mathbf{F}_{\rm ryd}(\mathbf{R},\,\mathbf{r}) = e\frac{\mathbf{R}}{R^3} + e\frac{\mathbf{r}-\mathbf{R}}{\left|\mathbf{r}-\mathbf{R}\right|^3}, \tag{4}$$

where e is the electron charge [16–18].

The last term in the adiabatic Hamiltonian (1) represents the interaction of the Rydberg atom and the diatomic molecule with the external electric field $\mathbf{F}_{\rm ext}$

$$H_{\rm ext} = e\mathbf{r}\cdot\mathbf{F}_{\rm ext} - \mathbf{d}\cdot\mathbf{F}_{\rm ext}. \tag{5}$$

Here, we consider an external electric field antiparallel along the LFF Z-axis with strength $F_{\rm ext}$, i.e., $\mathbf{F}_{\rm ext} = -F_{\rm ext}\hat{Z}$.

The total angular momentum of the triatomic molecule, but excluding an overall rotation, is given by $\mathbf{J} = \mathbf{l} + \mathbf{N}$, where $\mathbf{l}$ is the orbital angular momentum of the Rydberg electron. In the absence of the external electric field, the triatomic molecular states can be characterized by the projection of $\mathbf{J}$ along the LFF Z-axis, i.e., M_J. In the presence of the external field $\mathbf{F}_{\rm ext} = -F_{\rm ext}\hat{Z}$, there is azimuthal symmetry and M_J is conserved. In both cases, for $M_J \neq 0$, states with M_J and $-M_J$ are degenerate.

To solve the Schrödinger equation associated with the Hamiltonian (1), we perform a basis set expansion in terms of the coupled basis

$$\left|nlNJM_J\right\rangle = \Psi_{nlNJM_J}\left(\mathbf{r},\,\Omega_d\right) = \sum_{m_l=-l}^{m_l=l}\sum_{M_N=-N}^{M_N=N}\left\langle lm_lNM_N\middle|JM_J\right\rangle\psi_{nlm}(\mathbf{r})\times Y_{NM_N}\left(\Omega_d\right), \tag{6}$$

where $\langle lm_lNM_N|JM_J\rangle$ is the Clebsch–Gordan coefficient, $J = |l-N|,...,l+N$, and $M_J = -J,...,J$. $\psi_{nlm}(\mathbf{r})$ is the Rydberg electron wave function with n, l and m being the principal, orbital and magnetic quantum numbers, respectively. $Y_{NM_N}(\Omega_d)$ is the field-free rotational wave function of the diatomic molecule, with N and M_N being the rotational and magnetic quantum numbers, i.e., $Y_{NM_N}(\Omega_d)$ are the spherical harmonics. In the appendix, we explain how the Hamiltonian matrix elements in this coupled basis are computed.

In the following sections, we consider a Rydberg triatomic molecule formed by a rubidium atom and the diatomic molecule KRb. The rotational constant of KRb is $B = 1.114$ GHz [22], and its electric dipole moment $d = 0.566$ D [23]. We solve the Schrödinger equation belonging to the Hamiltonian (1) using the coupled basis

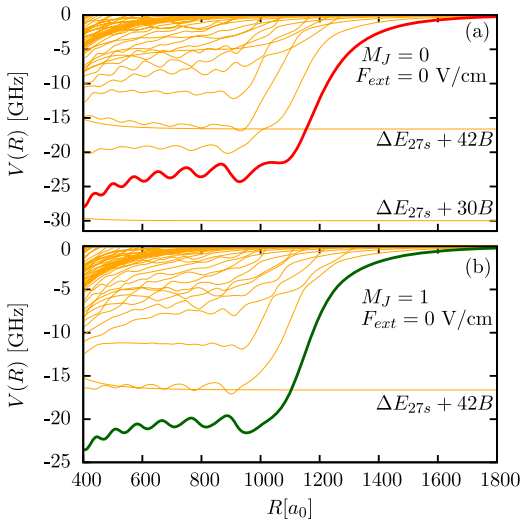

Figure 2. The Rb-KRb triatomic Rydberg molecule: BOPs as a function of the separation between the Rydberg core and the polar molecule R for (a) $M_J = 0$ and (b) $M_J = 1$. The calculations include the $27s$ state and the degenerate manifold $n = 24$ for $l \geqslant 3$ of rubidium. The energetically lowest lying states with $M_J = 0$ and 1 evolving from the $n = 24, l \geqslant 3$ manifold are plotted with thicker red and green lines, respectively. The zero energy has been set to the energy of the Rb($n = 24, l \geqslant 3$) degenerate manifold and the KRb ($N = 0$) level.

(6), which includes the Rb ($n = 24$, $l \geqslant 3$) degenerate manifold and the energetically closest neighboring Rydberg state $27s$. Note that we are neglecting the quantum defect of the $24f$ Rydberg state. For the diatomic molecule, we take into account the rotational excitations for $N \leqslant 6$.

3. The field-free BOPs and properties

In this section we investigate the BOP of the Rb-KRb triatomic molecule as a function of the separation R between KRb and Rb^+. The electric field induced by the Rydberg core and electron on the diatomic molecule decreases toward zero as R is increased. When the polar diatomic molecule is located far enough from the Rydberg ionic core and electron, the system could be considered as formed by two subsystems: a Rydberg atom and the diatomic molecule. Thus, the field-free asymptotic energy of the triatomic molecule is $E_{nl} + BN(N + 1)$, with N being the field-free rotational quantum number of the diatomic molecule and $E_{n,l}$ the energy of the Rydberg atom in a state with principal and orbital quantum numbers n and l, respectively.

For simplicity, and without loss of generality, this study is restricted to electronic states whose projections of the total angular momentum **J** along the LFF Z-axis are $M_J = 0$ and $M_J = 1$. Note that qualitatively similar results are obtained for BOPs with $M_J \geqslant 2$. In figures 2(a) and (b), we present the BOPs evolving from the Rb($n = 24$, $l \geqslant 3$) manifold with $M_J = 0$ and $M_J = 1$, respectively, as a function of R. Here, the zero energy has been set to the energy of the Rb($n = 24, l \geqslant 3$) degenerate manifold and the KRb($N = 0$) level. All the curves within a panel belong to triatomic molecular states with the same symmetry, and all the crossings between the BOPs are therefore avoided crossings.

Two different types of behavior are observed in figure 2. The BOPs of the triatomic molecule formed from the Rb($27s$) state and KRb in an excited state show a weak dependence on R. Their field-free limits are $\Delta E_{27s} + 30B$ and $\Delta E_{27s} + 42B$, with $\Delta E_{27s} = |E_{27s} - E_{24,3}|$, referring to KRb($N = 5, 6$) rotational excitations, respectively. In contrast, the BOP of the triatomic molecule formed from the Rb($n = 24, l \geqslant 3$) manifold possess an oscillatory behavior as a function of R. This reflects the dominant oscillatory behavior of the Rydberg electric field which is due to the oscillatory structure of the electronic Rydberg wave functions.

The lowest triatomic molecular states with $M_J = 0$ and $M_J = 1$ steming from the Rb($n = 24, l \geqslant 3$) Rydberg manifold are shifted more than 20 GHz for $R \lesssim 1200\ a_0$ and $1000\ a_0$, respectively. When R is increased beyond a certain limit, their energies increase and approach the field-free dissociation limit, Rb($n = 24, l \geqslant 3$) -KRb($N = 0$).

These results are converged with respect to the size of the basis set in (6). Table 1 contains the energies of the atomic Rydberg levels close to the Rb($n = 24, l \geqslant 3$) degenerate manifold. The energy gaps between the Rydberg levels are larger than the energy shifts of the levels evolving from this degenerate manifold observed in Rb-KRb, see figure 2. This justifies that only the next neighboring level $27s$ has to be included in the basis set. Further including the $25d$ and $26p$ states decreases the energy differences to less than 1%. It may be possible for the Rb-

Table 1. Atomic rubidium: energies and energy differences $\Delta E_{nl} = |E_{n,l} - E_{24,3}|$ of the Rydberg levels close to the degenerate Rydberg manifold $n = 24$ and $l \geqslant 3$.

n	l	$E_{n,l}$(THz)	ΔE_{nl}(GHz)
25	3	−5.26375	447.78
28	0	−5.31981	391.72
26	2	−5.41266	298.87
27	1	−5.54796	163.57
24	3	−5.71153	*0*
27	0	−5.77493	63.40
25	2	−5.87995	168.42
26	1	−6.03333	321.80

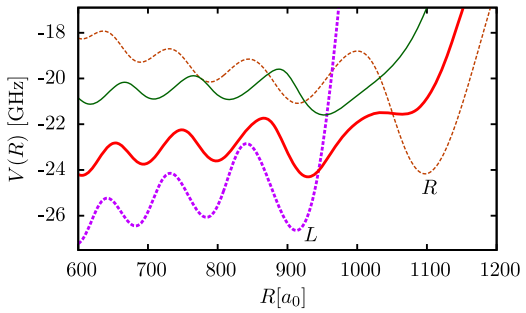

Figure 3. For the Rb-KRb triatomic molecule: BOPs derived using the two state model with states L (thick dashed line) and R (thin dashed line), and the rigid rotor description, levels with $M_J = 0$ (thick solid line) and $M_J = 1$ (thin solid line), of the diatomic molecule KRb. The differences between these two sets of BOPs show the importance of excited rotational states of the diatomic molecule which play a key role in the KRb rotational dynamics and in the level structure of the Rydberg triatomic molecule.

KRb triatomic molecular energy levels formed by the KRb diatomic molecule in highly excited rotational states and a Rb atom in lower lying Rydberg levels to provide BOPs within the spectral range of figure 2. However, the coupling of such triatomic molecular states to those presented in figure 2 would be very weak, due to the large rotational energy separation in KRb.

We have also checked the convergence of our results with respect to the number of rotational states of KRb included in the basis set. By increasing the number of rotational excitations from six to eight, the relative difference between the two sets of energies is smaller than 2×10^{-6}. This implies that BOPs obtained with the rotational basis including rotational excitations with $N \leqslant 6$ are well converged.

For comparison, we have also determined the BOP for a Rb-KRb triatomic molecule, but using a two-state approximation to describe the internal motion of the diatomic molecule KRb [18]. In the two-state model, the rotational energy gap is obtained from the rotational constant, $B = 1.114$ GHz, and the electric dipole moment is parallel to the LFF Z-axis so that KRb cannot freely rotate. Thus, we only consider the Z component of the electric field induced by the Rydberg atom $\mathbf{F}_{\text{ryd}}$ in equation (A.8). In figure 3, we present the energies of the two lowest states evolving from the Rb($n = 24, l \geqslant 3$) manifold using the two-state model and the rigid rotor description. The energy shift of these BOPs from the atomic Rb($n = 24, l \geqslant 3$) energy is smaller when the rigid rotor description is used. This could be due to the effect of the X and Y components of the electric field, which reduce the net effect of the Z component. The depth of the potential wells is also decreased, which implies that they will accommodate fewer vibrational levels. This effect is particularly pronounced for the lowest wells of the two-state triatomic molecule near $R \sim 920\ a_0$, and 1100 a_0 where the dipole is pointing toward and away from the ion core, respectively. When the rigid-rotor approximation is used, the outermost potential well near $R \sim 1100\ a_0$ is very shallow, and the diatomic molecule is also oriented away from Rb^+. In the two-state model these two BOPs have different symmetries and do cross, while the closest energy separation for the rigid rotor description is approximately 1.8 GHz. Furthermore, they are not coupled if an additional electric field is applied parallel to the Z-axis, see section 4. The significant differences between these two sets of results demonstrate that excited rotational states of KRb are involved and that the dynamical treatment of its rotational degree of freedom performed in this work is required for a proper description of the Rydberg triatomic system.

For a rotating molecule in an electric field, the pendular states appear for strong fields when it becomes oriented along the field direction; each pendular state being a coherent superposition of field-free rotational states [24]. For the diatomic KRb within the triatomic Rb-KRb, the electric field induced by the Rydberg core

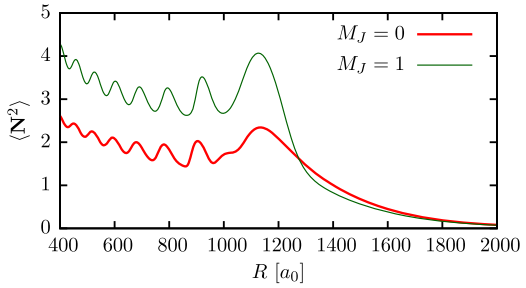

Figure 4. For the KRb diatomic molecule within the Rb-KRb Rydberg molecule, the expectation value $\langle \mathbf{N}^2 \rangle$ versus the separation R between the Rydberg core and KRb is shown for the lowest triatomic molecule electronic states with $M_J = 0$ and 1 evolving from the Rb $(n = 24, l \geqslant 3)$ degenerate manifold.

and electron should be expected to lead to these pendular levels. The strong hybridization of the angular motion of KRb is illustrated by the expectation value $\langle \mathbf{N}^2 \rangle$. For the lowest triatomic molecular states with $M_J = 0$ and 1 evolving from the Rb$(n = 24, l \geqslant 3)$ degenerate manifold, $\langle \mathbf{N}^2 \rangle$ is plotted as a function of R in figure 4. For both states, $\langle \mathbf{N}^2 \rangle$ oscillates reaching values well above the field-free one $\langle \mathbf{N}^2 \rangle = 0$. The fact that in both cases $\langle \mathbf{N}^2 \rangle$ surpasses the field-free value of the rotational state $N = 1$, i.e., $\langle \mathbf{N}^2 \rangle = 2$, indicates that higher rotational excitations contribute to the field-dressed rotational dynamics of KRb. Due to the complicated coupling mechanism between $\mathbf{l}$ and $\mathbf{N}$, any orbital angular momentum of the Rydberg electron could be combined with any rotational excitation of KRb to obtain a Rydberg trimer state with $M_J = 0$ or 1. The analysis of the field-dressed wave function indicates that at $R = 400\ a_0$ the rotational states with $N \leqslant 3$ and $N \leqslant 4$ have the largest contribution to the rotational dynamics of the electronic states with $M_J = 0$ and 1, respectively, and the weight of higher partial waves is smaller than 0.4%. Similar results are obtained for other values of R. For an isolated KRb molecule, we have computed the Stark effect of the rotational ground state [25], thereby showing that external electric fields of strengths 19 kV cm^{-1} or 50 kV cm^{-1} lead to a hybridization of the angular motion $\langle \mathbf{N}^2 \rangle > 1$ and 2, respectively, similar to the observed values in figure 4 for $R \lesssim 1400\ a_0$. As R is increased beyond 1200 a_0, the electric field strength is reduced and $\langle \mathbf{N}^2 \rangle$ decreases slowly approaching zero for $R \gtrsim 2000\ a_0$. This indicates that these states belong to the degenerate manifold formed by the $n^2 - 9$ levels of the Rydberg atom, i.e., $l \geqslant 3$, and KRb in its rotational ground state, i.e., $N = 0$. For alkali metal atoms in general, there are three Rydberg levels with appreciable quantum defects, s, p, and d levels, accounting for a total of $n^2 - 9$ hydrogenic levels.

The KRb molecule is strongly oriented and aligned due to the electric field induced by the Rydberg core and electron. The orientation and alignment of the diatomic molecule along the LFF Z-axis in the lowest triatomic molecular states with $M_J = 0$ and 1 for the Rb manifold $n = 24$ and $l \geqslant 3$, are illustrated by the expectation values $\langle \cos\theta_{dZ} \rangle$ and $\langle \cos^2\theta_{dZ} \rangle$ in figures 5(a) and (b), respectively. Since the Rydberg electric field has also components along the X- and Y-axes, we have also estimated the alignment of KRb along the LFF X-axis by means of $\langle \cos^2\theta_{dX} \rangle$in figure 5(c). Let us mention that the alignments along the Y- and X-axes are identical, i.e., $\langle \cos^2\theta_{dX} \rangle = \langle \cos^2\theta_{dY} \rangle$, and that the diatomic molecule does not gain any orientation along these axes, i.e., $\langle \cos\theta_{dX} \rangle = \langle \cos\theta_{dY} \rangle = 0$. For $R \lesssim 1000\ a_0$, the KRb within these two electronic states is strongly oriented toward the Rydberg core, $\langle \cos\theta_{dZ} \rangle$ oscillates as R is varied and $|\langle \cos\theta_{dZ} \rangle|$ shows a decreasing trend. This behavior can be explained in terms of the competition between the electric fields due to the electron and Rb^+ core. At these distances, the electric field due to the Rydberg core is dominant, then the total electric field along the Z-axis is pointing toward Rb^+, and KRb is anti-oriented. The dc-field due to the Rydberg electron oscillates resembling the behavior of its wave function, a pattern that is manifest in $\langle \cos\theta_{dZ} \rangle$ via its oscillatory behavior. As R is increased, the Rb^+ electric field decreases as R^{-2}, which explains that $|\langle \cos\theta_{dZ} \rangle|$ decreases correspondingly. For $R \gtrsim 900\ a_0$, the electric field produced by the electron becomes more important, some of its components are of the same order of magnitude as the contribution due to Rb^+, and, as a consequence, we observe an increase in the amplitude of the oscillations of $\langle \cos\theta_{dZ} \rangle$. For $R \gtrsim 1000\ a_0$, the electric field due to the Rydberg electron becomes dominant and the electric field along the Z-axis points away from Rb^+. Thus, the orientation of KRb is reversed and the dipole becomes oriented away from the Rydberg core. Around the classical turning point $R \sim 2n^2\ a_0 = 1152\ a_0$, the diatomic molecule achieves the maximal orientation with $\langle \cos\theta_{dZ} \rangle = 0.79$ and 0.61 for the $M_J = 0$ and 1 BOPs, respectively. In the laboratory a strong dc-field of 50 kV cm^{-1} is required to induce a large orientation $\langle \cos\theta_{dZ} \rangle = 0.8$ on the rotational ground state of an isolated KRb [25]. Thus, the electric field that KRb experiences at $R = 400\ a_0$ and 1152 a_0 in the $M_J = 0$ BOP is equivalent to 50 kV cm^{-1} in the lab. For $R > 2n^2 a_0$, the Rydberg triatomic molecule resembles a H_2^+ like system, in which the electron is localized between Rb^+ and KRb. By further increasing R, $\langle \cos\theta_{dZ} \rangle$ monotonically decreases and slowly approaches the field-free value $\langle \cos\theta_{dZ} \rangle = 0$. Note that even for $R \approx 2000\ a_0$ these states exhibit a weak orientation

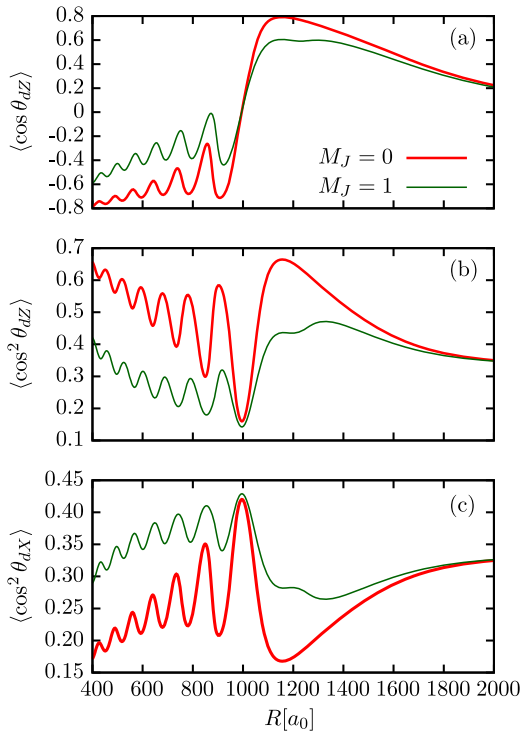

Figure 5. For the KRb diatomic molecule within the Rb-KRb triatomic Rydberg molecule, we show (a) the orientation $\langle\cos\theta_{dZ}\rangle$, (b) and (c) the alignment along the Z-axis $\langle\cos^2\theta_{dZ}\rangle$ and the X-axis $\langle\cos^2\theta_{dX}\rangle$, respectively, versus the separation between the Rydberg core and KRb. The results are presented for the triatomic molecular states with $M_J = 0$ (thick line) and $M_J = 1$ (thin line) evolving from the Rb($n = 24, l \geqslant 3$) degenerate manifold.

$\langle\cos\theta_{dZ}\rangle \approx 0.2$, which could be produced in an isolated KRb by applying an external dc field of 2.5 kV cm^{-1} in the lab. The alignment parameters, $\langle\cos^2\theta_{dZ}\rangle$ and $\langle\cos^2\theta_{dX}\rangle$ also show oscillatory behavior as R is varied. For the $M_J = 0$ state, the diatomic molecule is more aligned along the Z-axis than along the X-axis, i.e., $\langle\cos^2\theta_{dZ}\rangle > \langle\cos^2\theta_{dX}\rangle$. Whereas, for the $M_J = 1$ state, it holds that $\langle\cos^2\theta_{dZ}\rangle < \langle\cos^2\theta_{dX}\rangle$. For both states, at those values of R where $\langle\cos^2\theta_{dZ}\rangle$ reaches a maximum, $\langle\cos^2\theta_{dX}\rangle$reaches a minimum and vice versa. The smallest (largest) value of $\langle\cos^2\theta_{dZ}\rangle$ ($\langle\cos^2\theta_{dX}\rangle$) is obtained when $\langle\cos\theta_{dZ}\rangle \approx 0$, i.e., KRb changes from being oriented toward the Rb^+ core to away from it. The maxima and minima of $\langle\cos^2\theta_{dZ}\rangle$ and $\langle\cos\theta_{dZ}\rangle$ are reached at very close values of R.

For the $M_J = 1$ triatomic molecular state, $\langle\cos\theta_{dZ}\rangle$and $\langle\cos^2\theta_{dZ}\rangle$ reach a shallow minimum and $\langle\cos^2\theta_{dX}\rangle$ a maximum for $R \approx 1200\ a_0$ which are due to a very broad avoided crossing that this state experiences with a neighboring state. Note that in the behavior of $\langle\mathbf{N}^2\rangle$, this avoided crossing is not observed because both triatomic molecular states have similar values of $\langle\mathbf{N}^2\rangle$.

4. The electric field-dressed BOPs

Due to their enormous polarizabilities, Rydberg atoms are extremly sensitive to weak electric fields, i.e., a dc field of 10 V cm^{-1} significantly affects the Rydberg degenerate manifold $n = 24$ and $l \geqslant 3$ of rubidium. In contrast, the impact of such weak fields on the KRb rotational motion is negligible because the shift due to the external field, e. g., $dE_{\rm ext} \leqslant 3.1$ MHz for $F_{\rm ext} \leqslant 10$ V cm^{-1}, is much smaller than the rotational splitting. However, the electric field induced by the Rydberg ion and electron in the diatomic molecule is also significantly modified and, as consequence, the level structure of the triatomic Rydberg molecule and the BOP change correspondingly. Most importantly, the triatomic potentials evolving from the Rb($n = 24, l \geqslant 3$) Rydberg manifold acquire a substantial amount of s-wave character, which might allow for the creation of these giant polyatomic Rydberg molecules by the standard two-photon excitation of the ground-state atoms from a mixture of ultracold Rb atoms and KRb molecules [17]. In this section, we investigate the impact of an additional external electric field on the BOPs of the Rb-KRb triatomic molecule. For the sake of simplicity, we assume that this external field is antiparallel to the LFF Z-axis, i.e., $\mathbf{F}_{\rm ext} = -F_{\rm ext}\hat{Z}$, and focus on the weak field regime $F_{\rm ext} \leqslant 12$ V cm^{-1}. For a tilted external electric field, the azimuthal symmetry will be broken, and M_J will no longer be a good quantum number, substantially increasing the overall complexity.

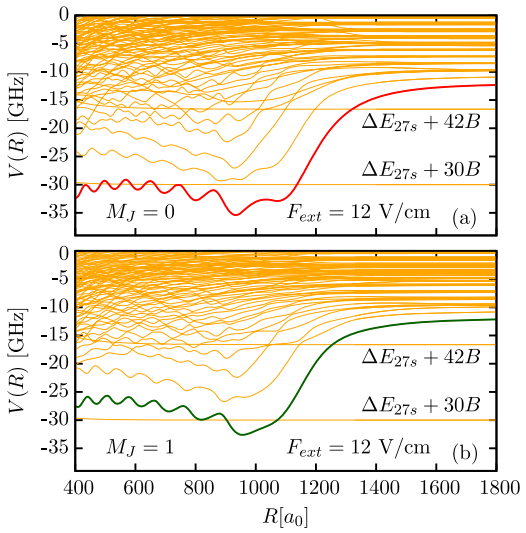

Figure 6. The Rb-KRb triatomic molecule in an external electric field $F_{\rm ext} = 12$ V cm^{-1}. BOPs as a function of the separation R between the Rydberg core and the polar molecule for (a) $M_J = 0$ and (b) $M_J = 1$ are shown. The calculations include the $27s$ state and the degenerate manifold $n = 24$ and $l \geqslant 3$ of rubidium. The lowest lying states with $M_J = 0$ and 1 evolving from the $n = 24$ and $l \geqslant 3$ manifold are plotted with thicker red and green lines, respectively. The zero energy has been set to the energy of the Rb($n = 24, l \geqslant 3$) degenerate manifold and the KRb($N = 0$) level in the absence of the external field as in figure 2.

In figures 6(a) and (b), we present the BOPs with $M_J = 0$ and 1, respectively, evolving from Rb($n = 24, l \geqslant 3$) for an external electric field strength $F_{\rm ext} = 12$ V cm^{-1}. The zero energy has been set to the energy of the Rb ($n = 24, l \geqslant 3$) degenerate manifold and the KRb($N = 0$) level in the absence of the external field as in figure 2. Comparing these field-dressed results to the field-free ones presented in figure 2, two different types of behavior are observed. The BOPs of the triatomic molecule formed from the Rb($27s$) state and KRb being in an excited rotational state are not affected by the external field, because the quadratic Stark effect of the $27s$ Rydberg state is very small. Since the Rb($n = 24, l \geqslant 3$) degenerate manifold is significantly affected by the external field, the BOPs evolving from this degenerate manifold and KRb($N = 0$) are also strongly affected. The energy of the electronic states is decreased by a few GHz. This reduction in energy depends on the separation between the Rb atom and the KRb molecule, and the smaller R the smaller this reduction is. These energy shifts can be explained in terms of the dominant contribution to the electric field that binds the Rydberg triatomic molecule: if it is due to the Rb^+ core they are smaller, whereas if it is due to the Rydberg electron they are larger reflecting the impact of the external field on the Rydberg wave function. The lowest BOP evolving from the Rb($n = 24, l \geqslant 3$) Rydberg manifold crosses the BOP from the Rb($27s$)-KRb($N = 5$) states, creating a sequence of avoided crossings, which are however very narrow due to the weak coupling between the involved states. Note that all the curves within a panel belong to triatomic molecular states with the same symmetry, and all the crossings between the BOP are therefore avoided crossings. Due to the external electric field, the degeneracy of the atomic Rydberg manifold Rb ($n = 24, l \geqslant 3$) is lifted, and for large separations between Rb^+ and KRb, the different BOP approach therefore different asymptotes.

We focus now on the evolution of the lowest BOP with $M_J = 0$ and 1, respectively, evolving from the Rb ($n = 24, l \geqslant 3$) manifold as the electric field strength $F_{\rm ext}$ is increased, see figures 7(a), (b). As the field becomes stronger, the BOPs are energetically lowered. As a consequence of the R-dependence of the overall electric field, the depth of the outermost potential well is slightly increased. This is particularly observed in the last two outer wells for the $M_J = 0$ BOP, where for $F_{\rm ext} \neq 0$ a highly-asymmetric double-well structure becomes visible.

The orientation of KRb is almost unaffected by these weak electric fields, see figure 8, because a few kV cm^{-1} are required to have a significant impact on the rotational dynamics of KRb [25]. For instance, an external field of $F_{\rm ext} = 50$ kV cm^{-1} would compensate the field due to the Rydberg core and electron at $R \sim 1100a_0$, and at this distance the KRb within the $M_J = 0$ BOP should not be oriented. However, such a strong electric field would ionize the Rydberg atom. Thus, it is only possible to control these giant Rydberg molecules by applying weak electric fields, that significantly affect the Rydberg electron wave function and, therefore, the adiabatic energy curves of the triatomic molecule and their vibrational structure as we will describe in the following section.

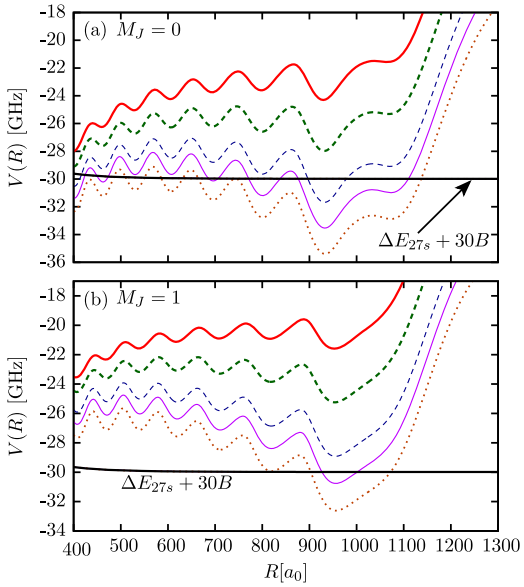

Figure 7. The Rb-KRb triatomic molecule in an external electric field. The lowest lying BOPs are shown for (a) $M_J = 0$ and (b) $M_J = 1$ evolving from the Rb($n = 24, l \geqslant 3$) Rydberg manifold as a function of the separation R between Rb^+ and KRb. The electric field strengths are $F_{\rm ext} = 0$ V cm^{-1} (thick solid), 4 V cm^{-1} (thick dashed), 8 V cm^{-1} (thin dashed), 10 V cm^{-1} (thin solid), and 12 V cm^{-1} (dotted).

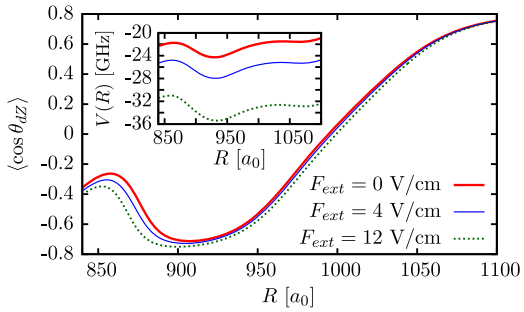

Figure 8. The Rb-KRb triatomic molecule in an external electric field for $F_{\rm ext} = 0, 4$ and 12 V cm^{-1}, the orientation $\langle \cos \theta_{dZ} \rangle$ of KRb within the lowest lying BOP with $M_J = 0$ evolving from the degenerate Rb ($n = 24$, $l \geqslant 3$) Rydberg manifold is shown. In the inset the energy of these BOP versus R is provided.

5. Vibrational states

One of the most important features of the adiabatic electronic potentials is the possibility to support vibrational levels in the wells in which these giant polyatomic Rydberg molecules would exist. In this section, we investigate the vibrational bound levels within the outer two minima of the BOP belonging to the lowest $M_J = 0$ triatomic molecular state evolving from the Rb($n = 24, l \geqslant 3$) degenerate manifold, in an external electric field of strength $F_{\rm ext} = 0, 4$ and 12 V cm^{-1}. The perturber molecule KRb within the Rb-KRb triatomic system is oriented toward the Rb^+ core in the inner (L) well, and becomes oriented away from it in the last shallow well, see figure 8. By increasing $F_{\rm ext}$, the orientation of KRb is only weakly affected, but the depth of the BOP is increased, which implies an enhancement of the number of bound vibrational levels. In figure 8, one can appreciate the shift between the minima in the BOP, and the maxima/minima in the orientation of the KRb diatomic molecule.

With no external field, the last (R) outer well potential is not deep enough to accommodate a bound state. In the inner potential well (L), there exists eight bound vibrational levels. In figure 9(a), we present the absolute square of the wave functions of these vibrational states. The expectation values $\langle R \rangle_\nu = \langle \psi_{\nu,0} | \, R \, | \psi_{\nu,0} \rangle$, with $\psi_{\nu,0} = \psi_{\nu,0}(R)$ being the vibrational wave functions, are presented versus the vibrational quantum number ν in figure 10. These vibrational bands, with an energy spacing of a few hundreds MHz, i.e., $|E_{\nu=1} - E_{\nu=0}| = 408$ MHz and $|E_{\nu=7} - E_{\nu=6}| = 183$ MHz, have superimposed rotational structure determined by the rotational constant $B_\nu = \langle R^{-2} \rangle_\nu / 2\mu$, of the order of a few tens of kHz, i.e., $B_0 = 40.2$ kHz and $B_7 = 37.5$ kHz.

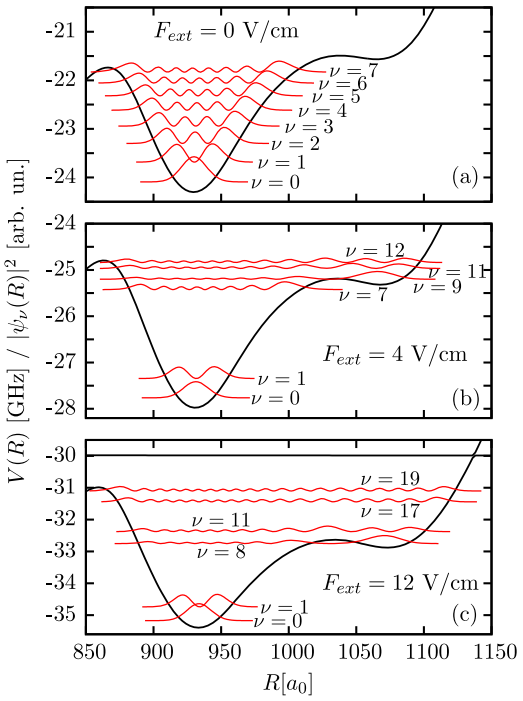

Figure 9. The modulus square of the wave functions $|\psi_\nu(R)|^2$ of several vibrational bound states within the last two wells of the energetically lowest BOP with $M_J = 0$ evolving from the degenerate Rb($n = 24, l \geqslant 3$) Rydberg manifold. The square of the wave functions are plotted in arbitrary units, and their positions are shifted to the energies of the corresponding vibrational state.

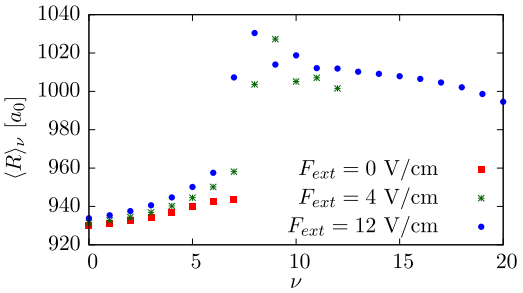

Figure 10. For an external electric field $F_{\rm ext} = 0, 4$ and 12 V cm^{-1}, we show the expectation value $\langle R \rangle_\nu$ of the vibrational bound states within the last two wells of the lowest BOP with $M_J = 0$ evolving from the degenerate Rydberg manifold, Rb($n = 24, l \geqslant 3$).

For $F_{\rm ext} = 4$ V cm^{-1}, there are 13 vibrational levels bound in the two outermost potential wells. Due to the presence of the external field, the last well becomes deeper and can accommodate vibrational levels, and accordingly we encounter in figure 9(b) a double-well structure. For instance, the wave functions of the states with vibrational quantum number $\nu = 8$,..., 12 extend over both wells with $\langle R \rangle_\nu > 1000\ a_0$, see figure 10. For $R \approx 1000\ a_0$, the orientation of KRb is close to zero, since its dipole is changing from being oriented toward the Rb^+ core to away from it. Thus, only for the $\nu = 9$ state, KRb is significantly oriented toward the Rydberg core. A similar energy spacing is found between neighboring vibrational levels as in the $F_{\rm ext} = 0$ V cm^{-1} case, except for the $\nu = 8$ and 9 states, which are 36 MHz apart.

By further increasing the field to $F_{\rm ext} = 12$ V cm^{-1}, the last two potential wells possess 20 vibrational levels. The vibrational wave function of the $\nu = 8$ state is partially contained in the outermost (R) well, see figure 9(c), having $\langle R \rangle_\nu \approx 1030\ a_0$, and at this distance the polar molecule is oriented away from the rubidium core. Highly excited vibrational states have $\langle R \rangle_\nu \approx 1000\ a_0$, and for similar separation distances, the KRb molecule does not present any orientation, see figure 8. The smallest vibrational spacing of 12.5 MHz is found between the $\nu = 7$ and 8 levels.

Due to the non-adiabatic interactions, the electronic states are hybridized allowing for intra-electronic dipole transitions. For instance, for $F_{\rm ext} = 12$ V cm^{-1} (4 V cm^{-1}) the vibrational levels $\nu = 0$ and $\nu = 8$ ($\nu = 9$)

could be coherently coupled in a Raman process via a highly excited vibrational state within this BOP as has been suggested in [16]. In such a way, the KRb orientation becomes entangled.

6. Conclusions

We have investigated ultralong-range triatomic Rydberg molecules formed by a Rydberg rubidium atom and the KRb diatomic rotational molecule in the presence of electric fields. The field effect arises from both the 'internal' Rydberg core and electrons and from an externally applied field. This species exhibits novel binding properties due to the attractive interaction of the Rydberg electron and the ground state KRb diatomic molecule, which can be controlled by an external field. Previous studies have modeled the diatomic molecule in a simple two level paradigm. We have been systematically extending this approach by taking into account the rotational motion of the diatomic molecule which couples, due to its dipole moment, to the electric field supplied by the Rydberg ionic core and the Rydberg electron or an external source. The rotational motion of the KRb diatomic molecule is described within the rigid rotor approximation, which allows for a proper description of the hybridization of the rotational motion of KRb due to the electric fields. The BOP curves for $M_J = 0,\ 1$ for the Rydberg triatomic molecule as a function of the separation between the Rb^+ core and the KRb diatomic molecule have been derived and analyzed. We have performed a detailed analysis of the hybridization of the angular motion, orientation and alignment of KRb within the Rb-KRb triatomic molecule. These results demonstrate that excited rotational states are involved in the field-dressed dynamics, and, therefore, the rotational degrees of freedom are needed for a proper description of the Rydberg triatomic molecule.

In an additional external electric field, the level structure of the Rydberg triatomic molecule is severely modified. The BOPs evolving from the Rb($n = 24, l \geqslant 3$) Rydberg manifold are strongly lowered, due to electronic hybridization, as $F_{\rm ext}$ increases, whereas those levels evolving from the non-degenerate Rb(27) state are weakly affected. The field-dressed potentials strengthen the bound state character of the rovibrational molecular states and lead for certain configurations to narrow avoided crossings. In the presence of an external field, a Raman scheme among different vibrational levels within the lowest electronic state evolving from the Rb ($n = 24, l \geqslant 3$) Rydberg manifold could be used to prepare entangled states of KRb levels with different orientations.

In an ultracold quantum gas which forms the KRb, there are typically as many potassium atoms as rubidium atoms. Hence, there are two options to form the triatomic Rydberg molecular states, i.e., K^*-KRb and Rb^*-KRb triatomic molecules. The main difference between the two highly excited triatomic molecules are the different low angular momentum states with appreciable quantum defects and energy levels of the Rydberg spectra of K and Rb, which provide a variable binding of the corresponding ground state heteronuclear diatomic molecule KRb. The two types of triatomic molecules do share the atomic (K or Rb) degenerate manifold such as the $n = 24$ and $l \geqslant 3$, as employed here. Thus, the BOPs emerging from the degenerate manifold are identical for both triatomic molecules since they only depend on the properties of the polar ground state diatomic molecule and the atomic Rydberg degenerate manifold under consideration. Their interaction (avoided crossings) with the quantum defect BOPs will, of course, move in energy and nuclear configuration space from one to the other species. Similar arguments hold for any other combination of Rydberg atoms and polar diatomic molecules possessing an electric dipole moment below the critical value $d_{\rm cr} = 0.639315$ a.u [26–29] above which the Rydberg electron would bind to the dipolar diatomic molecule.

For rubidium, the energy splitting of the neighboring levels of the $n = 24$ Rydberg manifold, a few tens of GHz, see table 1, is at least one order of magnitude larger than the rotational constant of KRb, $B = 1.114$ GHz, which determines the rotational energy splitting of a polar diatomic molecule. By rotationally exciting the diatomic molecule to $N = 7$, the rotational splitting to the $N = 8$ level is larger than 62 GHz, and close to the energy difference between the $27s$ level and the degenerate manifold $n = 24, l \geqslant 3$ of Rb. Thus, a regime could be achieved where the electronic degree of freedom of the Rydberg atom could be resonantly coupled to the rotational degree of freedom of the diatomic molecule. One could then imagine the opening of novel resonant decay processes, such as, e.g., Rydberg de-excitation of Rb and rotational excitation of KRb and vice versa. A detailed study of this regime and the existence of such resonant couplings and their characterization is however beyond the scope of this work.

An even more complete description of the triatomic Rydberg molecule would take into account the vibrational motion of the diatomic molecule. However, the energy scales involved into the vibrations are much larger than those of the rotation and therefore little impact of the electric field of either internal or external origin can be expected. Also, the coupling of the rotation to the vibration of the diatomic molecule should be negligible for sufficiently low-lying rovibrational states. The corresponding potential energy surfaces then become four-dimensional with three vibrational degrees of freedom from the field-free situation and the additional rotational degree of freedom which turns into a vibration for sufficiently strong fields.

Acknowledgments

RGF gratefully acknowledges a Mildred Dresselhaus award from the excellence cluster 'The Hamburg Center for Ultrafast Imaging Structure, Dynamics and Control of Matter at the Atomic Scale' of the Deutsche Forschungsgemeinschaft and financial support by the Spanish Ministry of Science FIS2011-24540 (MICINN), grants P11-FQM-7276 and FQM-4643 (Junta de Andalucía), and by the Andalusian research group FQM-207. We also acknowledge financial support by the Initial Training Network COHERENCE of the European Union FP7 framework. HRS and PS acknowledge ITAMP at the Harvard-Smithsonian Center for Astrophysics for support.

Appendix. The Hamiltonian matrix

In this appendix we describe how to compute the Hamiltonian matrix in the coupled basis $\langle nlNJM_J|\ H_{\rm mol}\ |n'l'N'J'M'_{J'}\rangle$. To determine the matrix elements $\langle nlm|\ \mathbf{F}_{\rm ryd}(\mathbf{R},\ \mathbf{r})|n'l\hat{a}m'\rangle$, we use the relation

$$\frac{\mathbf{r}-\mathbf{R}}{\left|\mathbf{r}-\mathbf{R}\right|^3}=\nabla_{\rm R}\frac{1}{\left|\mathbf{r}-\mathbf{R}\right|}, \tag{A.1}$$

where $\nabla_{\rm R}$ is the Laplacian with respect to the molecular coordinate $\mathbf{R}=(R\hat{R},\ \theta_R\hat{\theta},\ \phi_R\hat{\phi})$, see [30]. The electric field reads

$$\mathbf{F}_{\rm ryd}(\mathbf{R},\ \mathbf{r})=\frac{e\hat{Z}}{R^2}+e\sum_{l=0}^{\infty}\sqrt{\frac{4\pi}{2l+1}}\mathbf{A}_l(R,\ r,\ \Omega) \tag{A.2}$$

with

$$\mathbf{A}_l(R,\ r,\ \Omega)=\begin{cases}\dfrac{r^l}{R^{l+2}}\left[\dfrac{\sqrt{l(l+1)}}{2}Y_{l1}^{-}(\Omega)\hat{X}-\dfrac{i\sqrt{l(l+1)}}{2}Y_{l1}^{+}(\Omega)\hat{Y}-(l+1)Y_{l0}(\Omega)\hat{Z}\right] & \text{if}\quad r<R,\\ \dfrac{R^{l-1}}{r^{l+1}}\left[\dfrac{\sqrt{l(l+1)}}{2}Y_{l1}^{-}(\Omega)\hat{X}-\dfrac{i\sqrt{l(l+1)}}{2}Y_{l1}^{+}(\Omega)\hat{Y}+lY_{l0}(\Omega)\hat{Z}\right] & \text{if}\quad r>R,\end{cases} \tag{A.3}$$

where $\Omega=(\theta,\ \phi)$ and $\mathbf{r}=(r\hat{R},\ \theta\hat{\theta},\ \phi\hat{\phi})$ are the coordinates of the Rydberg electron, and

$$Y_{l1}^{\pm}(\Omega)=\Big(Y_{l1}(\Omega)\pm Y_{l-1}(\Omega)\Big). \tag{A.4}$$

In equation (A.3), $\mathbf{R}=R\mathbf{Z}$. The first two terms in expression (A.3) couple states with $\Delta m_l=\pm1$, which means that the projection m_l on the Z-axis is not conserved. In addition, the electric field induced by the Rydberg electron and the core is non-parallel to the Z-axis, implying that for the diatomic molecule M_N is not a good quantum number. The matrix elements of $\mathbf{F}_{\rm ryd}(\mathbf{R},\ \mathbf{r})$ in the Rydberg electron basis are given by

$$\langle nlm|\ \mathbf{F}_{\rm ryd}(\mathbf{R},\ \mathbf{r})|n'l'm'\rangle=F^X_{nlmn'l'm'}(R)\hat{X}+F^Y_{nlmn'l'm'}(R)\hat{Y}+F^Z_{nlmn'l'm'}(R)\hat{Z} \tag{A.5}$$

with

$$F^X_{nlmn'l'm'}(R)=e\sqrt{2\pi}\sum_{l''=|l-l'|}^{l+l'}\sqrt{2\pi}\sqrt{\frac{l''(l''+1)}{2l''+1}}\mathcal{R}_{l'',nln'l'}(R)\int_\Omega Y^*_{l'm'}(\Omega)Y^{-}_{l''1}(\Omega)Y_{lm}(\Omega)\,{\rm d}\Omega, \tag{A.6}$$

$$F^Y_{nlmn'l'm'}(R)=-ie\sqrt{2\pi}\sum_{l''=|l-l'|}^{l+l'}\sqrt{\frac{l''(l''+1)}{2l''+1}}\mathcal{R}_{l'',nln'l'}(R)\int_\Omega Y^*_{l'm'}(\Omega)Y^{+}_{l''1}(\Omega)Y_{lm}(\Omega)\,{\rm d}\Omega \tag{A.7}$$

and

$$F^Z_{nlmn'l'm'}(R)=\frac{e}{R^2}\delta_{nn'}\delta_{ll'}\delta_{mm'}+e\sum_{l''=|l-l'|}^{l+l'}\sqrt{\frac{4\pi}{2l''+1}}\mathcal{Z}_{l'',nln'l'}(R)\int_\Omega Y^*_{l'm'}(\Omega)Y_{l''0}(\Omega)Y_{lm}(\Omega)\,{\rm d}\Omega. \tag{A.8}$$

The integral in equation (A.8) ensures that $F^Z_{nlmn'l'm'}(R)$ is nonzero only if $|l-l'|\leqslant l''\leqslant l+l'$. The radial integrals take on the following appearance:

$$\mathcal{R}_{l'',nln'l'}(R)=\int_0^R\frac{r^{l''}}{R^{l''+2}}\psi^*_{n'l'}(r)\psi_{nl}(r)r^2{\rm d}r+\int_R^\infty\frac{R^{l''-1}}{r^{l''+1}}\psi^*_{n'l'}(r)\psi_{nl}(r)r^2{\rm d}r \tag{A.9}$$

$$\mathcal{Z}_{l'',nln'l'}(R) = -(l''+1)\int_0^R \frac{r^{l''}}{R^{l''+2}}\psi^*_{n'l'}(r)\psi_{nl}(r)r^2\mathrm{d}r + l''\int_R^\infty \frac{R^{l''-1}}{r^{l''+1}}\psi^*_{n'l'}(r)\psi_{nl}(r)r^2\mathrm{d}r, \quad \text{(A.10)}$$

where $\psi_{nl}(r)$ is the radial component of the Rydberg electronic wave function.

References

[1] Stebbings R F and Dunning F B (ed) 1983 *Rydberg States of Atoms and Molecules* (Cambridge: Cambridge University Press)
[2] Pethick C J and Smith H 2008 *Bose–Einstein Condensation in Dilute Gases* (Cambridge: Cambridge University Press)
[3] Killian T C, Pattard T, Pohl T and Rost J M 2007 *Phys. Rep.* **449** 77
[4] Pohl T, Adams C S and Sadeghpour H R(ed) 2011 Cold Rydberg gases and ultra-cold plasmas *J. Phys. B: At. Mol. Opt. Phys.* **44** 180201 (special issue)
[5] Weimer H, Müller M, Lesanovsky I, Zoller P and Büchler H P 2010 *Nat. Phys.* **6** 382
[6] Saffman M, Walker T G and Molmer K 2010 *Rev. Mod. Phys.* **82** 2313
[7] Greene C H, Dickinson A S and Sadeghpour H R 2000 *Phys. Rev. Lett.* **85** 2458
[8] Bendkowsky V, Butscher B, Nipper J, Shaffer J P, Löw R and Pfau T 2009 *Nature* **458** 1005
[9] Fermi E 1934 *Nuovo Cimento* **11** 157
[10] Omont A 1977 *J. Phys. France* **38** 1343
[11] Bendkowsky V *et al* 2010 *Phys. Rev. Lett.* **105** 163201
[12] Lesanovsky I, Sadeghpour H R and Schmelcher P 2007 *J. Phys. B: At. Mol. Opt. Phys.* **39** L69
[13] Kurz M, Mayle M and Schmelcher P 2012 *Europhys. Lett.* **97** 43001
[14] Kurz M and Schmelcher P 2013 *Phys. Rev.* A **88** 022501
[15] Krupp A T, Gaj A, Balewski J B, Hofferberth S, Löw R, Pfau T, Kurz M and Schmelcher P 2014 *Phys. Rev. Lett.* **112** 143008
[16] Rittenhouse S T and Sadeghpour H R 2010 *Phys. Rev. Lett.* **104** 243002
[17] Rittenhouse S T, Mayle M, Schmelcher P and Sadeghpour H R 2011 *J. Phys. B: At. Mol. Opt. Phys.* **44** 184005
[18] Mayle M, Rittenhouse S T, Schmelcher P and Sadeghpour H R 2012 *Phys. Rev.* A **85** 052511
[19] González-Férez R and Schmelcher P 2004 *Phys. Rev.* A **69** 023402
[20] González-Férez R and Schmelcher P 2005 *Phys. Rev.* A **71** 033416
[21] Marinescu M, Sadeghpour H R and Dalgarno A 1994 *Phys. Rev.* A **49** 982
[22] Ni K-K, Ospelkaus S, Nesbitt D J, Ye J and Jin D S 2009 *Phys. Chem. Chem. Phys.* **11** 9626
[23] Ni K-K, Ospelkaus S, de Miranda M H G, Pe'er A, Neyenhuis B, Zirbel J J, Kotochigova S, Julienne P S, Jin D S and Ye J 2008 *Science* **322** 231
[24] Friedrich B, Pullman D P and Herschbach D R 1991 *J. Phys. Chem.* **95** 8118
[25] González-Férez R, Mayle M, Sánchez-Moreno P and Schmelcher P 2008 *Eur. Phys. Lett.* **83** 43001
[26] Fermi E and Teller E 1947 *Phys. Rev.* **72** 399
[27] Turner J E 1977 *Am. J. Phys.* **45** 758
[28] Clark C W 1979 *Phys. Rev.* A **20** 1875
[29] Hotop H, Rul M-W and Fabrikant I I 2004 *Phys. Scr.* **2004** 22
[30] Ayuel K and de Chatel P 2009 *Physica* B **404** 1209